

## ADVANCES IN MATERIALS FOR ELECTROCATALYSIS<sup>1</sup>

S. Trasatti<sup>1</sup>

*Department of Physical Chemistry and Electrochemistry, University of Milan,  
Via Venezian 21, 20133 Milan, Italy*

### Abstract

Advances in research and development of materials for electrocatalysis are reviewed. After a scrutiny of the factors governing the electrocatalytic activity of materials and an analysis of the emerging trends, advances are illustrated by presenting recent unpublished results from the author's laboratory: H<sub>2</sub> evolution on Ni + RuO<sub>2</sub> composites, and on RhO<sub>x</sub> + RuO<sub>2</sub> anodes and cathodes for intermittent electrolysis, O<sub>2</sub> evolution on IrO<sub>2</sub> + SnO<sub>2</sub>, O<sub>2</sub> reduction on Co spinels prepared from different precursors.

*Keywords:* Electrocatalysis, oxide electrodes, hydrogen evolution, oxygen evolution, oxygen reduction, intermittent electrolysis.

### Introductory Concepts

Search for new or improved materials is restless in the field of electrochemistry. Materials are involved in power sources (batteries, fuel cells, capacitors) [1,2], in electrochemical reactors (electrodes for electrosynthesis, environmental processes, surface treatments) [3,4], as well as in various devices (sensors, electrochromic and electronic devices).

Electrical energy ( $\Delta V \times Q = \Delta V \times I \times t$ ) is produced in power sources and consumed in electrolyzers. Materials are needed to optimize the efficiency in the two cases: (a) maximum  $I$  with maximum  $\Delta V$  in power sources; (b) maximum  $I$  with minimum  $\Delta V$  in electrolyzers.  $\Delta V$  is the output voltage in (a) and the input voltage in (b).

Components of  $\Delta V$  are:

$$\Delta V = \Delta E \pm \Sigma \eta \pm IR \pm \Delta V_i \quad (1)$$

where the (+) sign is for electrolyzers and the (-) sign is for power sources.  $\Delta E$  is the thermodynamic (minimum) value (at  $I=0$ );  $\Sigma \eta$  is the sum of cathodic and anodic overpotentials;  $IR$  is the ohmic drop in the interelectrode gap, the electrodes and the connections,  $\Delta V_i$  simulates the stability, *i.e.*, deterioration with time of the other terms.

While  $\Delta E$  depends on the nature of the electrode reactions and cannot be changed without changing them,  $\eta$  depend typically on the electrode materials (assuming no mass transport limitations are operative). Therefore,  $\eta$  can be modified by changing electrode materials: this is the typical case of (heterogeneous) electrocatalysis.  $IR$  is essentially related to cell design: thus, it is

<sup>1</sup> From a lecture given at the XI Meeting of the Portuguese Electrochemical Society, 18-21 April 2001, Porto, Portugal.

more relevant to engineering (although the conductivity of electrode materials can have an impact). Finally, the stability is as a rule a typical problem of materials.

**Table 1**  
**Technological Demands**

- Improve the electrocatalytic activity for wanted reactions
- Depress the electrocatalytic activity for unwanted reactions
- Stabilize electrode materials toward wear
- Replace materials containing precious metals with (cheaper) materials based on non-precious metals
- Find substitute for polluting materials

Emphasis will be placed in this paper on materials for electrocatalysis. In this respect, research work is addressed to satisfy technological demands which are summarized in Table 1. In view of eqn. (1), electrodes for technological applications should satisfy the requirements listed in Table 2.

**Table 2**  
**Electrodes for Technological Applications**  
**Requirements**

- High surface area
- High electrical conduction
- Good electrocatalytic properties
- Long-term mechanical and chemical stability
- Minimized gas bubble problems
- Enhanced selectivity
- Availability and low cost
- Health safety

The main reactions for which electrocatalysis plays an essential role in technological applications are: Cl<sub>2</sub>, O<sub>2</sub> and H<sub>2</sub> evolution, O<sub>2</sub> and H<sub>2</sub> ionization, oxidation of organic molecules, as well as a number of environment-related reactions [5] listed in Table 3.

**Table 3**  
**Environment-Related Items**

- Water electrolysis (intermittent)
- SO<sub>2</sub> oxidation
- O<sub>3</sub> electrogeneration
- ClO<sub>2</sub> electrosynthesis
- CO<sub>2</sub> reduction
- H<sub>2</sub>O<sub>2</sub> direct synthesis
- Water pollutant degradation
- NO<sub>x</sub> destruction
- Chromate replacement in chlorate industry
- Desulfurization of natural gas
- CH<sub>4</sub> conversion
- On-site hypochlorite generation
- CN<sup>-</sup> destruction

<sup>††</sup> Fax: +39.02.26603-224; E-mail: trasatti@ici64.citca.it

The electrocatalytic activity is typically assessed on a relative basis. Reference electrode materials for the main electrode reactions are summarized in Table 4. These materials are a reference either because customarily used in technology, or because they exhibit ideal activity (eg, Pt). Various materials have already been tested for the various reactions, which can be grouped into general classes as tentatively indicated in Table 5. The largest variety of materials has been explored for H<sub>2</sub> evolution [6] and O<sub>2</sub> reduction [7,8]. The most common classes of materials are metals (present in all cases) and oxides (*idem*, except H<sub>2</sub> ionization). In this paper, attention will be focussed on oxides, for more than three decades investigated in the author's laboratory [9,10].

**Table 4**  
**Reference Electrode Materials**

- Hydrogen evolution: Ni, Fe, steel
- Oxygen evolution: Ni, Pb (Ag, Ca, Sn...)
- Oxygen reduction: Pt
- Chlorine evolution: DSA (mixed oxides)
- Hydrogen ionization: Pt

The enhancement of the electrode activity as electrode materials are replaced can be related either to *electronic factors* (chemical structure and composition of materials) or to *geometric factors* (surface area of materials). The former is a true electrocatalytic effect, the latter only an *apparent* electrocatalytic effect. Nevertheless, in technology both effects are welcome. The separation of the two effects is a target of R&D to be able to improve or optimize electrode materials. The immediate target of technology is to reduce  $\Sigma\eta$  in eqn. (1), whatever the way.

**Table 5**  
**Materials for Electrodes**

<i>Hydrogen evolution</i>	<i>Hydrogen ionization</i>	<i>Oxygen evolution</i>	<i>Oxygen reduction</i>	<i>Chlorine evolution</i>
Oxides	Metals	Oxides	Oxides	Oxides
Metals	Carbides	Metals	Metals	Metals
Alloys		Carbons		
Carbides		Macrocycles		
Sulphides				
Intermetallics				

A survey of the specific literature reveals that some general trends are the following: (a) Pursuing synergetic effects and (b) maximizing surface area. The former consists in using composite materials as well as in achieving more intimate mixing in mixed compositions. The latter is achieved by improving the physical dispersion of materials as well as by devising specific technology of preparation.

Emerging items in the preparation of electrocatalytic materials are summarized in Table 6. In particular high-energy ball milling can produce nanocrystalline materials [11], the same target of the sol-gel methodology [12] which however gives less striking results. Intermittent electrolysis is a

typical condition of electrolyzers powered by solar or eolian energy [13]. Gas diffusion electrodes are being extended more and more to electrolyzers [14,16]. Finally, the NEMCA (non Faradaic electrochemical modification of catalytic activity) is an effect discovered by Vayenas [17] which promises to be of high technological interest [18].

Table 6  
A Few Emerging Items

- Composite materials (metal, oxide, polymer matrix)
- Intermittent electrolysis
- Sol-gel methodology (surface area)
- High-energy ball milling (nanocrystalline materials)
- Gas diffusion electrodes (anodes and cathodes)
- NEMCA effect (electrochemical promotion)

In the field of electrocatalysis the author's laboratory has been active for several decades [19,23]. Targets have recently been: (a) study of new materials (metals, oxides, conducting polymers); (b) comparison of polycrystalline vs monocrystalline materials [24]; (c) synergetic effects in composite materials; (d) investigation of structure/activity relationships. In what follows a few specific cases will be illustrated.

#### Ni + RuO<sub>2</sub> Co-deposited Layers

In alkaline solution Ni is used as a cathode for H<sub>2</sub> evolution. Although chemically stable, its electrocatalytic activity is moderate and decreases progressively with use [5,6]. On the other hand RuO<sub>2</sub> is more active but more expensive [25]. Also, the mechanical stability of a RuO<sub>2</sub> film is lower. Thus, a composite material has been prepared comprising Ni and RuO<sub>2</sub>, obtained by electrodeposition of Ni from a Ni bath containing RuO<sub>2</sub> particles in suspension [26]. The target is to obtain a Ni electrode "pigmented" with RuO<sub>2</sub> particles embedded onto the Ni matrix and therefore mechanically stable.

Ni + RuO<sub>2</sub> were deposited from three different baths, identified by the main component, i.e., sulphate (Watts), chloride and thiosulphate, to investigate the effect of the composition of the bath. The amount of RuO<sub>2</sub> in suspension was varied between 0 and 10 g dm<sup>-3</sup>.

The occurrence of co-deposition was verified by SEM and XPS. Cyclic voltammetry showed that the presence of RuO<sub>2</sub> increases the surface charge. Sulphur was also deposited from the thiosulphate bath [27].

Fig. 1 shows that the activity of Ni cathodes is dramatically enhanced by the presence of RuO<sub>2</sub> particles, so much as to approach reversibility at low current densities. The Tafel slope decreases from ca. 100 mV, typical of Ni, to ca. 40 mV, typical of RuO<sub>2</sub>, already with 1-2 g dm<sup>-3</sup> RuO<sub>2</sub> in suspension. Although RuO<sub>2</sub> is expensive, the composite material with Ni contains a very small amount of precious compounds.

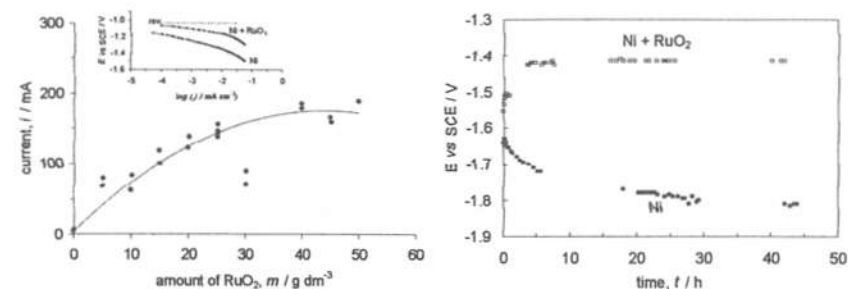


Figure 1 - Current density for H<sub>2</sub> evolution on Ni+RuO<sub>2</sub> composite materials vs amount of RuO<sub>2</sub> particles in the Ni bath. Inset: Tafel lines for H<sub>2</sub> evolution from alkaline solution. RuO<sub>2</sub> content in the bath: 10 g dm<sup>-3</sup>.

Figure 2 - Potential vs time at 100 mA cm<sup>-2</sup> for H<sub>2</sub> evolution from alkaline solution on Ni and Ni+RuO<sub>2</sub> composite material. RuO<sub>2</sub> content in the Ni bath: 10 g dm<sup>-3</sup>.

Fig. 2 shows that while Ni increases its overpotential with time, RuO<sub>2</sub> remains stable with a lower overpotential of 0.4 V. The stability of the composite material is also evident if the voltammetric charge of used samples is compared with that of fresh electrodes. A one-to-one correlation (unit slope) is clear indication of stability of the surface state of the composite sample.

While electrodes deposited from a Watts bath showed the best performance, lower activity was exhibited by those prepared from the thiosulphate bath, despite the good activity of sulphides in H<sub>2</sub> evolution [6].

#### Intermittent water electrolysis

Although electrolysis is a clean technology, it cannot be cleaner than the energy source used to power it. A truly ecological technology calls for a renewable energy source to power an electrolyzer. Solar and eolic energy conversions are the most advanced for applications. A problem with them is that the electrical energy provided is not constant but depends on natural events (winds, clouds, etc.). Therefore, electrolysis becomes unavoidably intermittent [28]. Intermittence produces more severe conditions for the stability of materials. Thus, special tests are required and *ad-hoc* materials have to be identified.

Intermittent electrolysis was simulated by appropriate current-time sequences. In the case of solar energy the change in power can be more sudden than in the case of eolic energy. Therefore, the current-time sequence was simulated by the current function illustrated in Fig. 3 where each step lasted 1 min and the maximum current was 200 mA cm<sup>-2</sup>. Fig. 3 shows that Ni+RuO<sub>2</sub> composite electrodes are stable under intermittent electrolysis and as active as pure RuO<sub>2</sub>.

Fig. 4 shows intermittent electrolysis with anodes. Co spinels are active materials *per se* [29]. If mixed with FeO<sub>x</sub> [30] their activity is enhanced. In particular, 10-15% FeO<sub>x</sub> produces the best activation, whereas other compositions are less active. On the basis of Figs. 3 and 4, water

intermittent electrolysis can profitably be carried out with a cathode of Ni+RuO<sub>2</sub> and an anode of NiCo<sub>2</sub>O<sub>4</sub> + 10% FeO<sub>x</sub>.

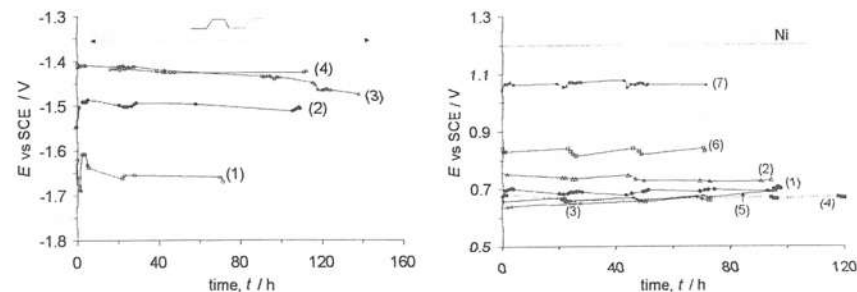


Figure 3 – Potential vs time at 100 mA cm<sup>-2</sup> for H<sub>2</sub> evolution from alkaline solution on Ni and Ni+RuO<sub>2</sub> composite materials in conditions of intermittent electrolysis. (1) Ni; (2) 2 g dm<sup>-3</sup>; (3) 10 g dm<sup>-3</sup> RuO<sub>2</sub>; (4) RuO<sub>2</sub>.

Figure 4 – Potential vs time at 200 mA cm<sup>-2</sup> for O<sub>2</sub> evolution from alkaline solution on Ni and NiCo<sub>2</sub>O<sub>4</sub>+FeO<sub>x</sub> composite materials in conditions of intermittent electrolysis. (1) NiCo<sub>2</sub>O<sub>4</sub>; (2) 5%; (3) 10%; (4) 15%; (5) 20%; (6) 40%; (7) 80% FeO<sub>x</sub>.

### Co<sub>3</sub>O<sub>4</sub>-based electrodes for O<sub>2</sub> reduction

O<sub>2</sub> reduction is important for fuel cells, batteries [31,32] as well as for electrolyzers (air cathodes [14,16], to decrease Δ*E* in eqn. (1)). In particular, in metal-air batteries the activation of carbon carriers with specific electrocatalysts can be different depending on the features of the power source. For mechanically rechargeable batteries, no bifunctionality is needed for the O<sub>2</sub> electrode (no O<sub>2</sub> evolution takes ever place); in this case, electrocatalysts need not be resistant to O<sub>2</sub> evolution and macrocycles can be used. In the case of electrochemically recharged batteries, bifunctional O<sub>2</sub> electrodes are necessary, although they may be less active for the specific reaction of O<sub>2</sub> reduction.

In the case of macrocycles of transition metals, those of Co [33] are usually the most active. The activity is particularly enhanced if macrocycles are subject to an appropriate pretreatment based on pyrolysis [34]. Analysis of the residues of pyrolysis reveals that Co oxide is present in the resulting material. Since macrocycles are expensive, we have investigated Co spinels as possible substitutes. In particular, we have scrutinized the effect of different precursors on the activity of the oxide obtained by thermal decomposition at 400 °C. Precursors were: Co nitrate, carbonate, citrate and oxalate. Previous studies [35] showed that the point of zero charge of the resulting oxide is the same, although morphological features differ substantially.

Oxides were prepared as powders, as films supported on Ni or mixed with carbon. Experiments of O<sub>2</sub> reduction were carried out in KOH solution. Materials were also tested with gas-diffusion electrodes in a pilot plant.

XRD and TEM revealed that Co<sub>3</sub>O<sub>4</sub> from carbonate is composed by particles with the

smallest size. The BET surface area was in fact the highest. The lattice constant is almost the same for all precursors, but the phase from the citrate contains also some CoO. The different particle sizes were also confirmed by different voltammetric charges, the highest being that of Co<sub>3</sub>O<sub>4</sub> from carbonate.

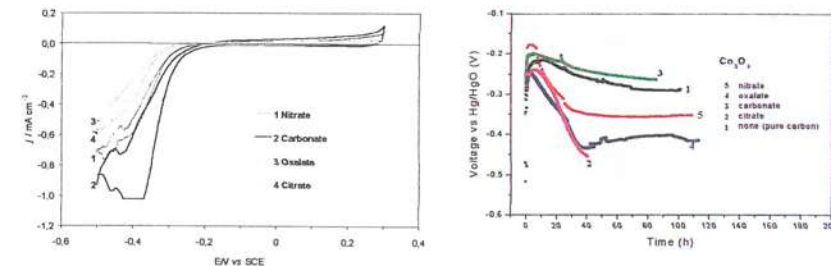


Figure 5 – Voltammetric curves in O<sub>2</sub> saturated solution of Co<sub>3</sub>O<sub>4</sub>-based electrodes prepared by thermal decomposition of different precursors. 1 mol dm<sup>-3</sup> KOH; Support: Ni. Active layer: 80 w % carbon + 20 w % oxide.

Figure 6 – Long-term performance of gas diffusion electrodes loaded with Co<sub>3</sub>O<sub>4</sub> prepared by thermal decomposition of different precursors. 7.5 mol dm<sup>-3</sup> KOH; 60 °C; 30 mA cm<sup>-2</sup>.

Fig. 5 shows voltammetric curves for O<sub>2</sub> reduction. The sequence of activity is carbonate > nitrate > citrate > oxalate. Fig. 6 shows the performance of electrodes in a pilot plant under operating conditions (60 °C, 7.5 mol dm<sup>-3</sup> KOH, 30 mA cm<sup>-2</sup>). While the oxide from nitrate is initially more active, that from carbonate is more stable and is the only one remaining more active than the pure carbon carrier.

Further experiments have shown that the pyrolysis of macrocycles still produces more active electrocatalysts. This means that synergetic effects are operative between the metal oxide and nitrogen moieties coming from the ligands. Experiments are now in progress to explore the possibility of synthesizing active catalysts from Co oxide precursors and nitrogen-containing compounds less expensive than macrocycles [36].

### IrO<sub>2</sub>-doped SnO<sub>2</sub> Anodes

Oxygen evolution in acid environment constitutes a very severe test for electrocatalysts. Only precious metal oxides are (relatively) stable [37]. Among these, IrO<sub>2</sub> is in principle the most resistant [38]. A practical problem is the cost of the precious compound. A possible solution is the use of composite materials where the precious compound is dispersed in a less active but more stable matrix.

Previous studies [39] have shown that IrO<sub>2</sub> + SnO<sub>2</sub> mixed oxides exhibit a strong surface enrichment with IrO<sub>2</sub>. In addition, mixing IrO<sub>2</sub> and SnO<sub>2</sub> together the surface charge of the resulting material is higher than for the pure oxides. Thus, IrO<sub>2</sub> + SnO<sub>2</sub> electrodes were prepared by thermal

decomposition of  $\text{Ir}(\text{NO}_3)_3$  and  $\text{SnCl}_2$  at 400 °C on Ti as a support.  $\text{O}_2$  evolution was studied in  $\text{HClO}_4$  solution.

Fig. 7 shows that the addition of  $\text{IrO}_2$  to  $\text{SnO}_2$  decreases the Tafel slope from 120 mV to ca. 60 mV, typical of  $\text{IrO}_2$ . Fig. 8 shows that the activity for  $\text{O}_2$  evolution increases with the  $\text{IrO}_2$  content by a factor of almost 500. It is clear that  $\text{IrO}_2$  is the active component and the sharp increase in activity is related to the strong surface enrichment with the precious metal oxide. Comparison of the voltammetric charge for fresh electrodes with that for aged electrodes shows that the composite materials are very stable under  $\text{O}_2$  evolution from acid solution.

In conclusion,  $\text{IrO}_2$  dominates the properties of the mixed oxides from 10 mol%. The highest activity is achieved with a  $\text{IrO}_2$  nominal content of  $\geq 20$  mol%, which reduces the cost of the anodes substantially.

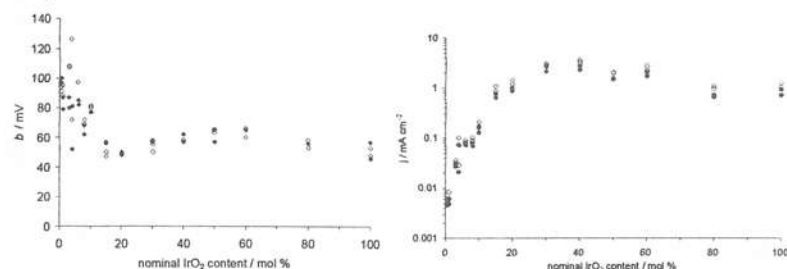


Figure 7 – Tafel slope as a function of  $\text{IrO}_2$  content for  $\text{O}_2$  evolution from acid solution on  $\text{IrO}_2+\text{SnO}_2$  mixed oxide electrodes. (○) Forward and (●) backward potential scan.

Figure 8 – Apparent current density at  $E = 1.5$  V (SHE) as a function of  $\text{IrO}_2$  content for  $\text{O}_2$  evolution from acid solution on  $\text{IrO}_2+\text{SnO}_2$  mixed oxide electrodes. (○) Forward and (●) backward potential scan.

### RhO<sub>x</sub>-based Electrodes

Precious metal oxides have been shown to be active for  $\text{H}_2$  evolution [21,25]. In particular, they are more stable and less sensitive to metallic impurities than metal electrodes. While results are available for  $\text{RuO}_2$  and  $\text{IrO}_2$  both in alkaline and in acid solutions, no data are available for  $\text{RhO}_x$ , although occasional results have shown that it is more active than other precious compounds.

$\text{RhO}_x$  electrodes on Ti were prepared by thermal decomposition at 400-600 °C of  $\text{RhCl}_3$  hydrate [40].  $\text{H}_2$  evolution was studied in  $\text{H}_2\text{SO}_4$  solution. Voltammetric curves show that  $\text{RhO}_x$  is probably reduced by  $\text{H}_2$  evolution, although it retains its stability. The voltammetric curve after  $\text{H}_2$  evolution exhibits a shape which resembles that of the pure metal [41], with a region of hydrogen adsorption/desorption and unsymmetrical peaks of surface oxidation/reduction. However, after reduction, the electrode becomes much more active for  $\text{H}_2$  evolution, which suggests that the reduction of the oxide probably produces a finely dispersed form of metallic Rh particles, something like a "Raney" [6] Rh, even if the entire oxide phase is not reduced.

Fig. 9 shows steady-state potentiostatic curves. The forward curve for the lower temperature

oxide exhibits a step at about -0.25 V (SCE), which is probably related to oxide reduction. In fact, the backward curve remains flat, with a very low Tafel slope which indicates hydrogenation of the surface. This is clearly evident in Fig. 10 showing the dependence of the Tafel slope on the temperature of calcination. The value for the forward and the backward curves converge toward a common value at the highest temperature, while as the temperature decreases the Tafel slopes diverge with a very low backward value.

It is interesting that if the activity ( $j$ ) is normalized to the unit of surface concentration of active sites ( $j/q^*$ , where  $q^*$  is the voltammetric charge), the normalized activity remains low up to ca. 500 °C and then increases dramatically. This probably indicates that the activity is dominated by geometric effects at low temperatures, and by electronic effects at higher temperatures.

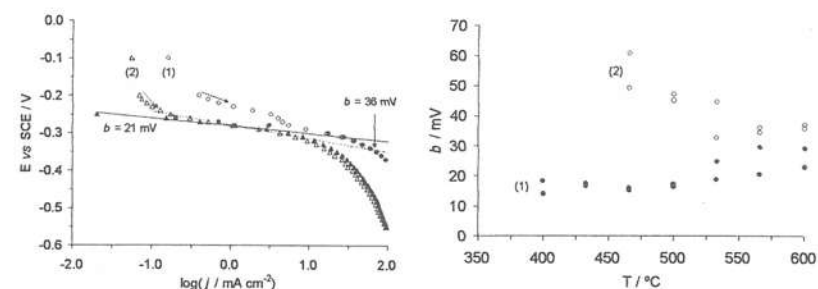


Figure 9 – Tafel lines for  $\text{H}_2$  evolution from acid solution on  $\text{RhO}_x$  electrodes prepared by thermal decomposition at different temperatures. (1) 430 °C; (2) 530 °C. Open symbols: Forward potential scan. Solid symbols: Backward potential scan.

Figure 10 – Tafel slope for  $\text{H}_2$  evolution from acid solution on  $\text{RhO}_x$  electrodes prepared at different calcination temperatures. (1) Forward and (2) backward potential scan.

### RhO<sub>x</sub> + RuO<sub>2</sub> Mixed Oxide Electrodes

Fig. 11 shows a comparison among  $\text{RhO}_x$ ,  $\text{RuO}_2$  and  $\text{IrO}_2$  for  $\text{H}_2$  evolution in acid media. The activity varies in the order  $\text{RhO}_x > \text{IrO}_2 > \text{RuO}_2$ . Since both  $\text{RhO}_x$  and  $\text{IrO}_2$  are much more expensive than  $\text{RuO}_2$ , it is certainly of interest to try to reduce the amount of  $\text{RhO}_x$  by mixing it with  $\text{RuO}_2$ . Therefore, mixed oxides were prepared by thermal decomposition of  $\text{RhCl}_3$  and  $\text{RuCl}_3$  hydrates at 400 °C.

XPS analysis has shown that there is some surface enrichment with  $\text{RuO}_x$  with a maximum of about 20% at 50 mol%. SEM analysis has shown that the morphology does not change visibly with composition, although the layer appears without cracks at intermediate Rh contents, whereas it is cracked near pure  $\text{RhO}_x$ . Voltammetric curves indicate that the surface charge is much higher for pure Rh oxide than Ru oxide. However, the charge increases up to 20%  $\text{RhO}_x$ , shows a maximum there, then increases steadily and dramatically for  $\text{RhO}_x > 50\%$ . At the same time the voltammetric curves suggest that  $\text{RhO}_x$  is presumably reduced as the Rh content is  $\geq 60\%$ .

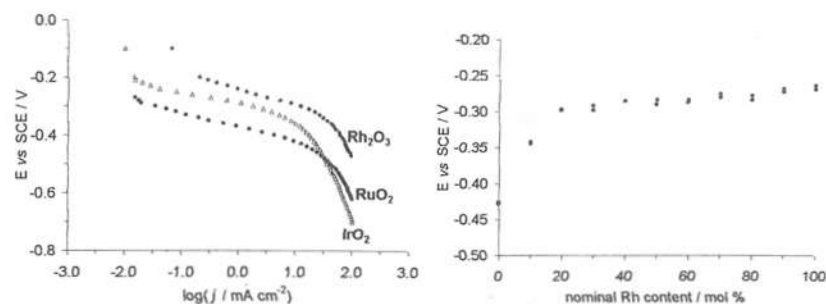


Figure 11 – Typical Tafel lines for H<sub>2</sub> evolution from acid solution on IrO<sub>2</sub>, RuO<sub>2</sub> and RhO<sub>x</sub> prepared by thermal decomposition at 400 °C.

Figure 12 – Potential at 3 mA cm<sup>-2</sup> as a function of the RhO<sub>2</sub> content of RuO<sub>2</sub>+RhO<sub>x</sub> mixed oxide electrodes for H<sub>2</sub> evolution from acid solution.

Fig. 12 shows that the potential at constant current decreases (lower overpotential) as the RhO<sub>x</sub> content increases. In particular, the potential decreases by ca. 0.15 V as only 20 mol% RhO<sub>x</sub> is added. Thus, the maximum activity is achieved with only 1/5 of Rh, with a substantial decrease in the cost of the electrode.

**Acknowledgements.** The author thanks the following co-workers for their contribution: A.C. Tavares, D. Milani, C. Mocchi, M. Bregolato, M. Campari, C.P. De Pauli. Financial support from M.U.R.S.T., C.N.R. and E.C.C. is gratefully acknowledged.

**References**

1. J. De Silvestro and O. Haas, *J. Electrochem. Soc.* **137** (1990) 5c.
2. B. E. Conway, *Electrochemical Supercapacitors*, Kluwer Academic/Plenum, New York, 1999.
3. K. Rajeshwar, J. G. Ibanez and G. M. Swain, *J. Appl. Electrochem.* **24** (1994) 1077.
4. A. M. Couper, D. Pletcher and F. C. Walsh, *Chem. Rev.* **90** (1990) 837.
5. S. Trasatti, *Int. J. Hydrogen Energy* **20** (1995) 835.
6. S. Trasatti in *Advances in Electrochemical Science and Engineering*, H. Gerischer and C. W. Tobias Eds., VCH, Weinheim, 1992, p.1.
7. E. Yeager, *Electrochim. Acta* **29** (1984) 1527.
8. C. Fischer, N. Alonso-Vante, S. Fiechter and H. Tributsch, *J. Appl. Electrochem.* **25** (1995) 1004.
9. S. Trasatti and G. Buzzanca, *J. Electroanal. Chem.* **29** (1971) App. 1.
10. S. Trasatti and G. Lodi in *Electrodes of Conductive Metallic Oxides*, S. Trasatti Ed., Part A, Elsevier, Amsterdam, 1980, p. 301.
11. L. Roué, D. Guay and R. Schultz, *J. Electroanal. Chem.* **480** (2000) 64.
12. Y. Murakami, S. Tsuchiya, K. Yahikozawa and Y. Takasu, *Electrochim. Acta* **39** (1994) 651.
13. J. W. Hollenberg, E. N. Chen, K. Lakeram and D. Modroukas, *Int. J. Hydrogen Energy* **30**

- (1995) 239.
14. N. Furuya and H. Aikawa, *Electrochim. Acta* **45** (2000) 4251.
15. N. Furuya and N. Mineo, *J. Appl. Electrochem.* **20** (1990) 475.
16. T. Morimoto, K. Suzuki, T. Matsubara and N. Yoshida, *Electrochim. Acta* **45** (2000) 4257.
17. C. G. Vayenas, S. Bebelis and S. Ladas, *Nature* **343** (1990) 625.
18. S. Wodiunig, F. Bokeloh, J. Nicole and Ch. Comninellis, *Electrochem. Solid-State Lett.* **2** (1999) 281.
19. S. Trasatti, *J. Electroanal. Chem.* **111** (1980) 125.
20. S. Trasatti and W.E. O'Grady in *Advances in Electrochemistry and Electrochemical Engineering*, H. Gerischer and P. Delahay Eds., Vol. 13, Interscience, New York, 1980, p. 177.
21. S. Trasatti in *Electrochemical Hydrogen Technologies*, H. Wendt Ed., Elsevier, Amsterdam (1990), pp. 1, 104.
22. S. Trasatti in *The Electrochemistry of Novel Materials*, J. Lipkowski and P. N. Ross Eds., VCH Publishers Inc., 1994, p. 207.
23. S. Trasatti in *Interfacial Electrochemistry: Theory, Practice, Applications*, A. Wieckowski Ed., Marcel Dekker, New York, 1999, p. 769.
24. L. M. Doubova, S. Trasatti, *J. Electroanal. Chem.* **467** (1999) 164.
25. S. Trasatti in *Modern Chlor-Alkali Technology*, T. C. Wellington Ed., Elsevier Applied Science, Amsterdam, 1992, p. 281.
26. A. B. Tavares and S. Trasatti in *Modern Chlor-Alkali Technology*, Vol. 7, S. Sealey Ed., The Royal Society of Chemistry, London, 1998, p. 65.
27. A. C. Tavares and S. Trasatti, *Electrochim. Acta*, **45** (2000) 4195.
28. G. Schiller, R. Henne, P. Mohr and V. Peinecke, *Int. J. Hydrogen Energy* **23** (1998) 761.
29. R. N. Singh, J. P. Pandey, N. K. Singh, B. Lal, P. Chartier and J.-F. Koenig, *Electrochim. Acta* **45** (2000) 1911.
30. N. Krstajić and S. Trasatti in *Proceedings of the Symposium on "Oxygen Electrochemistry"*, Vol. 95-26. The Electrochemical Society, Pennington, 1996, p. 155.
31. R. W. Reeve, P. A. Christensen, A. Hamnett, S. A. Haydock and S. C. Roy, *J. Electrochem. Soc.* **145** (1998) 3463.
32. H. Arai, S. Müller and O. Haas, *J. Electrochem. Soc.* **147** (2000) 3584.
33. A. L. Bouwkamp-Wijnoltz, W. Visscher and J. A. R. van Veen, *Electrochim. Acta* **39** (1994) 1641.
34. M. Ladouceur, G. Lalande, D. Guay, J. P. Dodelet, L. Dignard-Bailey, M. L. Trudeau and R. Schulz, *J. Electrochem. Soc.* **140** (1993) 1974.
35. S. Ardizzone, G. Spinolo and S. Trasatti, *Electrochim. Acta* **40** (1995) 2683.

36. S. Gupta, D. Tryk, I. Bae, W. Aldred and E. Yeager, *J. Appl. Electrochem.* **19** (1989) 19.
37. Ch Comminellis and G. P. Vercesi, *J. Appl. Electrochem.* **21** (1991) 335.
38. V. V. Gorodetskii, V. A. Neberchilov and M. M. Pecherskii, *Russ. J. Electrochem.* **30** (1994) 916.
39. C. P. De Pauli and S. Trasatti, *J. Electroanal. Chem.* **396** (1995) 161.
40. Yu. E. Roginskaya, O. V. Morozova, G. I. Kaplan, R. R. Shifrina, M. Smirnov and S. Trasatti, *Electrochim. Acta* **38** (1993) 2435.
41. M. I. Florit, A. E. Bolzán and A. J. Arvia, *J. Electroanal. Chem.* **394** (1995) 253.

## CHEMICAL AND ELECTROCHEMICAL CHARACTERIZATION OF COBALT BEARING FERRITES ORIGINATING FROM THE PURIFICATION OF COBALT CONTAINING WASTEWATER

E. Barrado<sup>1</sup>, F. Prieto<sup>2</sup>, F.J. Garay<sup>1</sup>, J. Medina<sup>3</sup> and M. Vega<sup>1</sup>

<sup>1</sup> Departamento de Química Analítica, <sup>3</sup> Departamento de Física de la Materia Condensada, Cristalografía y Mineralogía; Facultad de Ciencias, Universidad de Valladolid, 47005 Valladolid (SPAIN). E-mail: ebarrado@qa.uva.es

<sup>2</sup> Centro de Investigaciones Químicas, Universidad Autónoma del Estado de Hidalgo, Crta. Pachuca-Tulancingo, Km 4.5, 42076 Pachuca, Hidalgo (MEXICO).

### Abstract

In this research, the efficiency of the "ferrite process" for the purification of wastewater heavily contaminated with Cobalt (99.99% in the optimal conditions) was verified, and the three cobalt-bearing ferrites produced using three different Fe<sup>2+</sup>/Co<sup>2+</sup> molar ratios (15/1, 7/1 and 3/1) were characterized by chemical analysis (ICP-AES and potentiometric titration), XRF, XRD and DSC, indicating Co<sub>x</sub>Fe<sup>II</sup><sub>1-x</sub>Fe<sup>III</sup><sub>2</sub>O<sub>4</sub> (x = 0.16, 0.35, and 0.65 respectively) as the most probable structure of the solids. Electrochemical analysis of the solid cobalt ferrites was performed using a carbon paste electrode in HClO<sub>4</sub> and HCl media. In each case, the first cyclic-voltammogram showed the participation of solid species in the electrochemical transformation process. In second and successive scans, the voltammograms indicated the redox couples Fe<sup>3+</sup><sub>ads</sub> + 1e<sup>-</sup> ⇌ Fe<sup>2+</sup><sub>ads</sub> (E = 0.525 V vs. AgCl/Ag) and Co<sup>2+</sup> + 2e<sup>-</sup> ⇌ Co(s) (E = -0.230 V) in HClO<sub>4</sub>, and FeCl<sub>2</sub><sup>+</sup><sub>ads</sub> + 1e<sup>-</sup> ⇌ FeCl<sup>+</sup><sub>ads</sub> + Cl<sup>-</sup> (E = 0.475 V) and CoCl<sub>x</sub><sup>(x-2)-</sup> + 2e<sup>-</sup> ⇌ Co(s) + x Cl<sup>-</sup> (E = -0.320 V) in HCl.

**Keywords:** Cobalt, Wastewater treatment; Metal removal, Cobalt-ferrites, Voltammetry, Carbon paste electrode.

### INTRODUCTION

Uncontrolled industrial and agricultural practices, combustion processes and mining have led to the accumulation of toxic heavy elements into the environment [1,2]. The growing concern of increasing environmental levels has prompted rigorous restriction